

Ice flux divergence anomalies on 79north Glacier, Greenland

H. Seroussi,^{1,2} M. Morlighem,^{1,2} E. Rignot,^{1,3} E. Larour,¹ D. Aubry,² H. Ben Dhia,² and S. S. Kristensen⁴

Received 4 March 2011; revised 1 April 2011; accepted 3 April 2011; published 7 May 2011.

[1] The ice flux divergence of a glacier is an important quantity to examine because it determines the rate of temporal change of its thickness. Here, we combine high-resolution ice surface velocity observations of Nioghalvfjærdssjøen (79north) Glacier, a major outlet glacier in north Greenland, with a dense grid of ice thickness data collected with an airborne radar sounder in 1998, to examine its ice flux divergence. We detect large variations, up to 100 m/yr, in flux divergence on grounded ice that are incompatible with what we know of the glacier surface mass balance, basal mass balance and thinning rate. We examine the hypothesis that these anomalies are due to the three-dimensional flow of ice around and atop bumps and hollows in basal topography by comparing the flux divergence of three-dimensional numerical models with its surface equivalent. We find that three-dimensional effects have only a small contribution to the observed anomalies. On the other hand, if we degrade the spatial resolution of the data to 10 km the anomalies disappear. Further analysis shows that the source of the anomalies is not the ice velocity data but the interpolation of multiple tracks of ice thickness data onto a regular grid using a scheme (here block kriging) that does not conserve mass or ice flux. This problem is not unique to 79north Glacier but is common to all conventional ice thickness surveys of glaciers and ice sheets; and fundamentally limits the application of ice thickness grids to high-resolution numerical modeling of glacier flow. **Citation:** Seroussi, H., M. Morlighem, E. Rignot, E. Larour, D. Aubry, H. Ben Dhia, and S. S. Kristensen (2011), Ice flux divergence anomalies on 79north Glacier, Greenland, *Geophys. Res. Lett.*, 38, L09501, doi:10.1029/2011GL047338.

1. Introduction

[2] Significant changes in ice sheet mass balance have been observed in the past decades that are mainly caused by the rapid evolution of outlet glaciers at the periphery of ice sheets [Rignot and Kanagaratnam, 2006]. To understand and model these dynamic changes, advanced, high-resolution numerical models are needed because standard model simplifications, such as the Shallow Ice Approximation (SIA), cannot explain these observations. These advanced models must operate at a higher spatial resolution compatible with the size and thick-

ness (less than 1 km) of these glaciers to capture critical dynamical processes that drive their temporal evolution. In addition, these models must rely on data assimilation techniques to constrain unknown model parameters such as basal friction under grounded ice and ice viscosity of floating shelves [e.g., Joughin *et al.*, 2009; Morlighem *et al.*, 2010].

[3] The time evolution of the glacier thickness is dictated by the conservation of mass, which says that the temporal change in ice thickness is the difference between the net mass balance of the glacier (i.e., surface mass balance plus basal mass balance) and the volume flux divergence. When conducting temporal simulations of ice flow, it is important to examine the flux divergence because it controls the temporal evolution of ice thickness.

[4] Here, we analyze the ice flow of Nioghalvfjærdssjøen Glacier, hereby abbreviated 79north, a major outlet glacier in northeast Greenland. Several reasons guide us to study this glacier. First, we have comprehensive data on ice velocity from satellite radar interferometry (InSAR) [Rignot *et al.*, 1997]; second, this glacier was extensively surveyed in the late 1990s [Thomsen *et al.*, 1997; Christensen *et al.*, 2000], hence procuring a dense array of ice thickness and surface elevation. The glacier drains an area of 120,000 km² and forms an extensive (20 km × 80 km), relatively thin floating ice tongue at its northern junction with the Arctic Ocean. 79north is the largest discharger of ice in north Greenland, it branches out with Zachariæ Isstrøm and Storstrømmen glaciers from the northeast ice stream, a major, unique glaciological feature in Greenland that initiates near the summit of the ice sheet [Fahnestock *et al.*, 2001b]. It was suggested that this glacier could accelerate in response to ongoing retreat of sea-ice in this region and attendant effects on ice shelf stability [Reeh *et al.*, 2001]. At present, the glacier exhibits low flow speeds by Greenland standards (1 km/yr), and altimetry surveys show only small changes in glacier thickness since 1993 [Thomas *et al.*, 2006], i.e., the glacier is close to a state of mass equilibrium.

[5] We investigate the flux divergence of 79north and discuss its observed spatial patterns. We compare the results with outputs from numerical models of glacier flow, the quality of the ice velocity data and ice thickness data. Based on the results, we make recommendations on the gridding of ice thickness maps for ice sheet modeling studies.

2. Data and Methods

[6] The ice surface elevation and ice thickness of 79north were mapped extensively in July 1997 and 1998 during several airborne surveys [Thomsen *et al.*, 1997; Christensen *et al.*, 2000]. About 3,000 km of high quality radar thickness and laser altimetry data were collected with differential GPS positioning. The laser elevations have a precision of 10–20 cm. The precision of the bedrock elevation is limited

¹Jet Propulsion Laboratory, California Institute of Technology, Pasadena, California, USA.

²Laboratoire MSSMat, UMR 8579, CNRS, École Centrale Paris, Châtenay-Malabry, France.

³Department of Earth System Science, University of California, Irvine, California, USA.

⁴DTU-Space, Technical University of Denmark, Kongens Lyngby, Denmark.

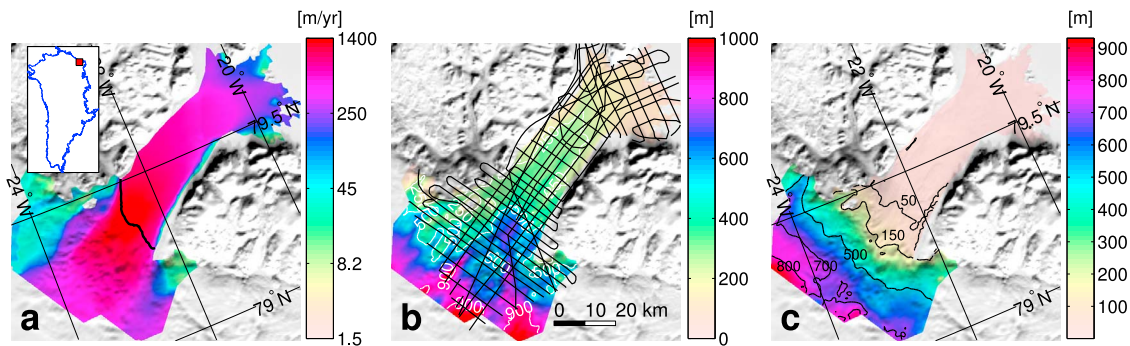


Figure 1. Characteristics of 79north Glacier, Greenland (inset map): (a) Ice velocity (m/yr) measured from ERS-1/2 InSAR color coded on a logarithmic scale and overlaid on a MODIS (Moderate-resolution Imaging Spectroradiometer) mosaic of Greenland; (b) Reeh’s gridded thickness data, color coded on a linear scale, with flight tracks indicated as black lines, and (c) Reeh’s surface elevation data. Ice flow is from the south to the north (top of the plot). The black line in Figure (a) delineates the grounding line, with floating ice to the north, grounded ice to the south.

by the nature of ice sounders (Doppler focused radars): the echo interpreted as bedrock may not originate from a point directly underneath the sensor. The track spacing of the radio echo sounding lines is 5 km on the relatively flat part of the glacier, and 2.5 km near the grounding zone [Thomsen *et al.*, 1997; Reeh *et al.*, 1999; Mayer *et al.*, 2000] (Figure 1b). Gridded thickness and surface elevation were generated at a 1-km posting by N. Reeh (unpublished) using block kriging, hereby referred to as Reeh’s thickness map.

[7] With InSAR data from the Earth Remote Sensing Satellite 1 and 2 (ERS-1/2), we mapped the grounding line position of 79north with a precision of ± 50 m in 1996, and its horizontal vector velocity at a spatial resolution of 50 m and a precision of 20 m/yr [Rignot *et al.*, 1997] (Figure 1a). The model domain of our study is constrained by the geographic limits of Reeh’s thickness map.

[8] The depth-integrated mass balance equation relates the temporal evolution of ice thickness, $\partial H/\partial t$, to the surface mass balance, \dot{M}_s (positive for accumulation, negative for ablation), the bottom mass balance, \dot{M}_b (positive when freezing, negative when melting), and the flux divergence:

$$\frac{\partial H}{\partial t} = -\nabla \cdot (\bar{\mathbf{u}}H) + \dot{M}_s + \dot{M}_b \quad (1)$$

where $\bar{\mathbf{u}}$ is the depth-averaged velocity. Surface mass balance values in our study domain range from -120 cm/yr at low elevation to -50 cm/yr at high elevation according to Ettema *et al.* [2009]. Temporal changes in ice thickness are comparatively small and less than a few 10 cm/yr [Thomas *et al.*, 2006].

[9] As a first approximation, we assume that the surface velocity of the glacier is equal to the depth-averaged ice velocity, i.e., $\mathbf{u}_s = \bar{\mathbf{u}}$, a valid assumption if the glacier is sliding entirely on its bed. Alternatively, we calculate the three dimensional velocity using a finite element model. Here, we employ the Ice Sheet System Model (ISSM) [Morlighem *et al.*, 2010]. We use an unstructured isotropic triangular mesh, with an element size of about 800 m, which is vertically extruded in 10 layers forming a 3D prismatic finite element mesh. We create two models that use two approximations of the momentum balance equation: 1) the higher-order Blatter/Pattyn (BP) model [Blatter, 1995; Pattyn, 2003], and 2) a full-Stokes (FS) solution.

[10] We assume that the ice follows Glen’s flow law. The ice sheet thermal regime is calculated using the conservation of energy equation assuming that the glacier is in a thermal steady-state. We impose air temperature at the surface from Fausto *et al.* [2009] and a constant geothermal flux of 42 mW/m^2 [Fahnestock *et al.*, 2001a]. From the thermal regime, we calculate the ice rigidity of grounded ice using Paterson [1994].

[11] To best fit the observed surface velocity, we infer two unknown parameters: 1) basal friction on grounded ice and 2) the depth-averaged rigidity on floating ice [Joughin *et al.*, 2009; Morlighem *et al.*, 2010]. To ensure that the models do not overfit the data and are not affected by observation noise, we add a Tikhonov regularization term [Vogel, 2002].

3. Results

[12] Figure 2a shows the flux divergence calculated from the Reeh’s ice thickness map and the ERS-1 InSAR velocity. The results reveal large, complex deviations, up to ± 100 m/yr, on grounded ice and large but more uniform variations, up to ± 50 m/yr, on floating ice. On the ice shelf, the flux divergence averages -50 m/yr near the grounding zone, which is consistent with the calculated average bottom melt rate of the ice shelf in steady-state [Rignot *et al.*, 2001]. The results also reveal the presence of elongated channels of preferred melting spreading from the grounding zone northwards, that are aligned with the main flow direction of ice, i.e., similar in nature to the features observed on the floating ice tongue of Petermann Gletscher [Rignot and Steffen, 2008]. The flux divergence decreases downstream, which is consistent with the decrease in ice shelf melting farther away from the grounding line, on the thinner part of the ice shelf.

[13] On grounded ice, the variations in flux divergence do not follow simple patterns, are more randomly structured, and exhibit both negative and positive values of larger magnitude than on floating ice. Anomalies exceed 100 m/yr in many areas. Such high values are neither compatible with the rates of thickness change, nor with the net surface mass balance that are two orders of magnitude smaller and would not exhibit such a high spatial variability. Basal melting of grounded ice should be orders of magnitude lower as well [Fahnestock *et al.*, 2001a]. The pattern of flux divergence is

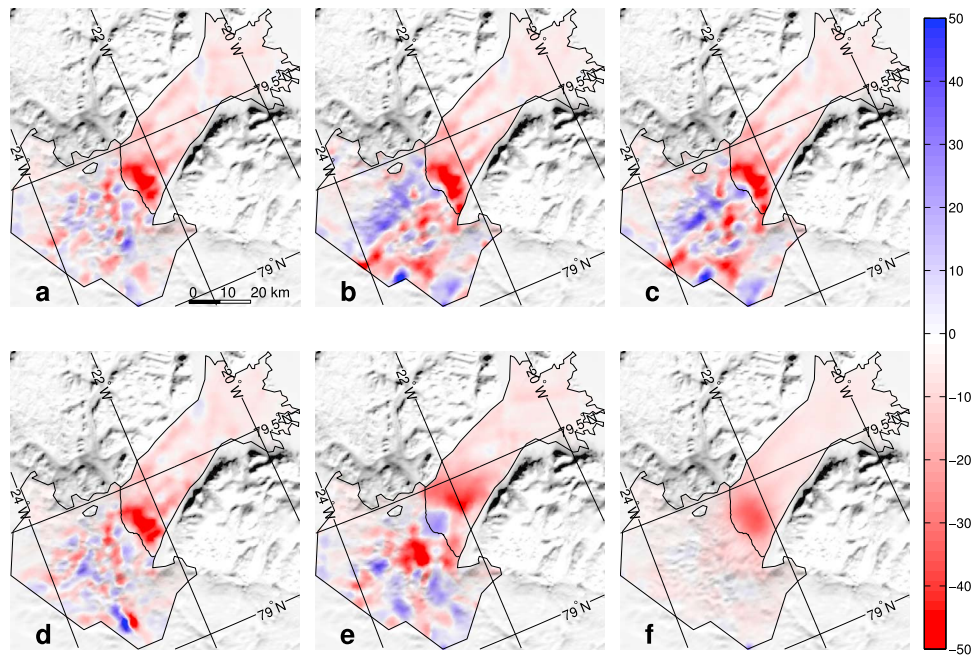


Figure 2. Ice flux divergence in m/yr of 79north Glacier, Greenland, calculated from (a) ERS-1 1996 ice velocity, (b) 3D Blatter-Pattyn model, (c) 3D full Stokes model, (d) RADARSAT-1 2000 ice velocity and Reeh's unpublished 1-km gridded thickness; (e) ERS-1 1996 ice velocity and Bamber's 5-km gridded thickness, and (f) ERS-1 velocity and Reeh's thickness degraded to 10 km resolution. The grounding line is a black line. Values are truncated to ± 50 m/yr to maintain visibility. Color-coded divergence values are overlaid on a MODIS mosaic of Greenland.

therefore incompatible with the known physical processes controlling changes in ice thickness.

[14] We now examine the flow simulations obtained using the 3D models which do not assume that the surface velocity is equal to the depth-averaged velocity. The misfit between the two 3D models and the surface observations averages 14 m/yr, i.e., the models are able to reproduce the surface velocities with great fidelity. On areas of fast flow, i.e., where velocity is > 50 m/yr, we find that $\|\bar{\mathbf{u}}\|/\|\mathbf{u}_s\|$ averages 99.0% for BP and 98.9% for FS. Peak-to-peak variations in this ratio do not exceed 4% within the ice stream, but larger deviations exist in slow-moving sectors along the margins. Overall, the average difference between surface and depth-averaged velocity is at the 1% level over the entire domain. This was expected as most of the ice in our domain is sliding over the bed.

[15] The flux divergence calculated from the 3D models (Figures 2b and 2c) is very similar to the one obtained with the surface velocity. Hence, the 3D flow of ice around and atop bumps and hollows in basal topography does not have a significant influence on the observed anomalies in flux divergence. It is also a reasonable assumption to use surface velocities to calculate the flux divergence. The anomalies are either due to errors in the velocity data or the thickness data.

[16] To examine ice velocity, we compare the results obtained with two mappings, at two epochs, with two different satellites, one using ascending and descending interferometric phase data from ERS-1/2 in year 1996 [Rignot *et al.*, 1997], and another using speckle tracking data from RADARSAT-1 in year 2000. The corresponding flux divergence in Figure 2a and 2d are similar, especially on the

fast flowing portion of the glacier, so the spatial pattern of divergence anomalies is robust across ice motion processing schemes.

[17] If we use a thickness map with a 5-km grid spacing from Bamber *et al.* [2001], the anomalies are still present but the spatial pattern is different (Figure 2e). Finally, if we degrade the spatial resolution of both ice velocity and ice thickness to 10 km, by using an averaging filter of 10 km in width, the anomalies are completely removed (Figure 2f). The 10 km value is consistent with the greatest separation between tracks of 5 km, which implies that gradients are only known with a resolution of 10 km. When smoothing is operated at 5 km, most anomalies re-appear. The anomalies are therefore caused by the ice thickness data.

[18] The flux divergence may be re-written as follows:

$$\nabla \cdot (\bar{\mathbf{u}}H) = H \nabla \cdot \bar{\mathbf{u}} + \bar{\mathbf{u}} \cdot \nabla H \quad (2)$$

Our observations indicate that the first term on the right hand side varies more strongly over short distances than the second term (Figure 3). The highest values of $\nabla \cdot \bar{\mathbf{u}}$ coincide with surface depressions, i.e., areas experiencing a significant variation in driving stress. This effect is reflected in the ice velocity data which are available at a high spatial resolution.

[19] The second term of the equation should compensate for these variations in velocity divergence but the thickness gradients are available at a resolution of only 5 km near the grounding line and 10 km away from the grounding line. Block kriging acts as a low-pass filter that tends to smooth out details and extreme values of the original dataset: differences between measurements and interpolated values locally exceed several tens of meters along flight tracks. It is

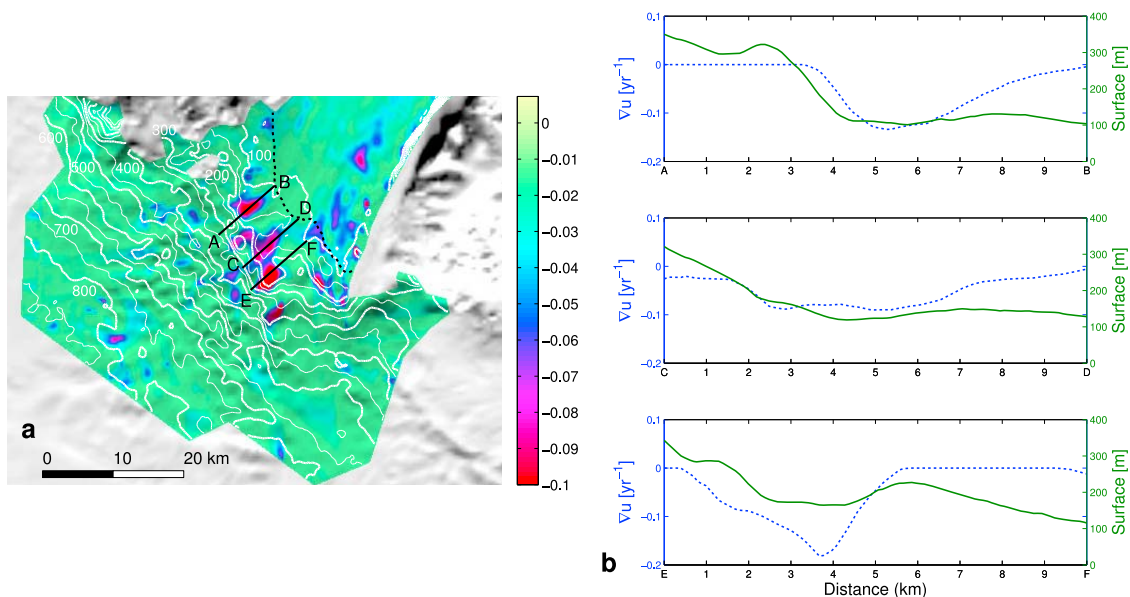


Figure 3. (a) Velocity divergence ($\nabla \cdot \mathbf{u}$, in m/yr) of 79north Glacier from ERS-1/2 InSAR velocities, overlaid on a MODIS mosaic with iso contours every 50 m (thin white lines) and 100 m (thick white lines). (b) Velocity divergence (blue dotted line) and surface elevation (green line, courtesy of I. Howat, 2011) along the 3 profiles A-F noted in Figure 3a.

therefore not possible for ice thickness to compensate for the high-resolution velocity gradients present in the velocity map. This results in severe anomalies in flux divergence.

4. Discussion

[20] Ice thickness is measured along single tracks with a high vertical precision (15 m) and spatial resolution (typically 20 m), but the flight tracks are spaced by 2.5 to 5 km. The original resolution of the data is therefore no better than 5 km. Our results demonstrate that this interpolation is not suited for the derivation of flux divergence at a resolution better than 10 km because the kriging of ice thickness at a finer sample spacing does not conserve ice flux and introduces anomalies in the flux divergence.

[21] Numerical ice flow models initiated with a flux divergence as in Figure 2a will rapidly diverge to a significantly different glacier configuration in the first time steps as the initial rates of change in thickness will be high. If instead the model assumes that these anomalies represent unknown, non-necessarily physical rates of bottom melting, i.e., $\dot{M}_b = \nabla \cdot (\bar{\mathbf{u}}H)$, the behavior of the time evolutive model may be biased and the results will be questionable.

[22] A first solution is to run the model at 10 km resolution. Several studies have however pointed out the need to operate numerical models at a higher spatial resolution [Vieli and Payne, 2005; Nowicki and Wingham, 2008], preferably close to one ice thickness, here 600 m. At 10 km resolution, bumps and hollows in bed topography that may slow or accelerate the retreat or advance of the glacier are smoothed out, small glaciers a few km in width cannot be modeled, and the high-resolution information along the ice thickness tracks is discarded. This approach is not compatible with the requirements of advanced high-resolution ice sheet models.

[23] A second solution is to increase the number of flight tracks to progressively converge toward, a 500-m spacing between tracks that will enable ice sheet modeling on a 1 km

grid. This would limit the errors in ice thickness to measurement errors as no kriging or interpolation will be required. This would require 5 times more data than already collected on this glacier, which is already one of the most thoroughly surveyed glaciers in Greenland. This approach is costly and probably impractical if it had to be extended to many other glaciers in Greenland.

[24] A third solution is to employ survey techniques that map the bed at high-resolution in 3D instead of along flight tracks. Novel 3D mapping techniques using radar tomography and interferometry techniques have been developed [Paden *et al.*, 2010]. These techniques provide high-resolution (100 m) data on 10 km wide swaths, but they have been tested mostly over flat, undisturbed parts of the ice sheet. We do not know how well they may work on the more challenging environment of steep, entrenched, deep outlet glacier troughs with rough surface topography, large englacial, supraglacial and subglacial heterogeneities, and complex reflections from reflectors off nadir.

[25] A fourth and probably most preferable solution is to devise a method of ice thickness gridding that conserves mass or ice flux, i.e., employ an algorithm that is more physically based. We will present one algorithm in a forthcoming paper.

[26] Regardless of the solution adopted, it is important to stress that the anomalies in flux divergence reported here are not unique to 79north but should be common to any glacier for which ice thickness grids are generated by interpolation of single track data, i.e., the majority of ice thickness surveys up to present. Our analysis demonstrates that this approach is not compatible with the requirements of high-resolution ice sheet models. The problem will be exacerbated on faster moving glaciers, which are also those of greater importance in controlling the evolution of ice sheet discharge because the magnitude of the anomalies scales with the velocity (Equation (2)). On Jakobshavn Glacier, which flows 10 times faster than 79north Glacier, vertical strain rates are 10 times larger and ice thickness is 3–4 times larger, so the anomalies in flux

divergence exceed ± 500 m/yr. It is clearly essential to devise new gridding techniques that do not rely on single tracks data but combine these data with other information, for instance ice velocity. Until such techniques are developed and employed, the use of gridded thickness maps in high-resolution 3D modeling of glacier flow should be treated with caution.

5. Conclusion

[27] In this study, we show that the combination of InSAR-derived, high-resolution surface velocities with gridded ice thickness maps of a well-surveyed glacier in north Greenland yields strong anomalies in ice flux divergence over grounded ice that are not physically tenable and fundamentally limit the capability of high-resolution, time-evolutionary ice sheet numerical models. These anomalies do not reflect complexities in the 3D flow of ice over a complex bed topography, but the shortcomings of commonly-used interpolation schemes for ice thickness that do not conserve mass. The anomalies are large enough to call into question the applicability of these thickness maps to high-resolution, high-order modeling of glacier flow.

[28] **Acknowledgments.** This work was performed at the Jet Propulsion Laboratory, California Institute of Technology, at the Department of Earth System Science, University of California Irvine and at Laboratoire MSSMat, École Centrale Paris, under a contract with the National Aeronautics and Space Administration, Cryospheric Sciences Program. We thank Ian Howat for providing surface elevation data, Jesse Johnson and an anonymous reviewer for helpful and insightful comments. This study was initiated under the precious guidance and leadership of Niels Reeh.

[29] The Editor thanks Jesse Johnson and an anonymous reviewer for their assistance in evaluating this paper.

References

- Bamber, J. L., R. L. Layberry, and S. P. Gogineni (2001), A new ice thickness and bed data set for the Greenland ice sheet: 1. Measurement, data reduction, and errors, *J. Geophys. Res.*, *106*, 33,773–33,780.
- Blatter, H. (1995), Velocity and stress-fields in grounded glaciers: A simple algorithm for including deviatoric stress gradients, *J. Glaciol.*, *41*(138), 333–344.
- Christensen, E. L., N. Reeh, R. Forsberg, J. H. Jørgensen, N. Skou, and K. Woelders (2000), A low-cost glacier-mapping system, *J. Glaciol.*, *46*(154), 531–537.
- Ettema, J., M. R. van den Broeke, E. van Meijgaard, W. J. van de Berg, J. L. Bamber, J. E. Box, and R. C. Bales (2009), Higher surface mass balance of the Greenland ice sheet revealed by high-resolution climate modeling, *Geophys. Res. Lett.*, *36*, L12501, doi:10.1029/2009GL038110.
- Fahnestock, M., W. Abdalati, I. Joughin, J. Brozena, and P. Gogineni (2001a), High geothermal heat flow, basal melt, and the origin of rapid ice flow in central Greenland, *Science*, *294*(5550), 2338–2342.
- Fahnestock, M. A., I. Joughin, T. A. Scambos, R. Kwok, W. B. Krabill, and S. Gogineni (2001b), Ice-stream-related patterns of ice flow in the interior of northeast Greenland, *J. Geophys. Res.*, *106*, 34,035–34,045.
- Fausto, R. S., A. P. Ahlstrøm, D. van As, S. J. Johnsen, P. L. Langen, and K. Steffen (2009), Improving surface boundary conditions with focus on coupling snow densification and meltwater retention in large-scale ice-sheet models of Greenland, *J. Glaciol.*, *55*(193), 869–878.
- Joughin, I., S. Tulaczyk, J. Bamber, D. Blankenship, J. Holt, T. Scambos, and D. Vaughan (2009), Basal conditions for Pine Island and Twaites Glaciers, West Antarctica, determined using satellite and airborne data, *J. Glaciol.*, *55*(190), 245–257.
- Mayer, C., N. Reeh, F. Jung-Rothenhauser, P. Huybrechts, and H. Oerter (2000), The subglacial cavity and implied dynamics under Nioghalvfjærdssjorden Glacier, NE-Greenland, *Geophys. Res. Lett.*, *27*(15), 2289–2292.
- Morlighem, M., E. Rignot, H. Seroussi, E. Larour, H. Ben Dhia, and D. Aubry (2010), Spatial patterns of basal drag inferred using control methods from a full-Stokes and simpler models for Pine Island Glacier, West Antarctica, *Geophys. Res. Lett.*, *37*, L14502, doi:10.1029/2010GL043853.
- Nowicki, S. M. J., and D. J. Wingham (2008), Conditions for a steady ice sheet-ice shelf junction, *Earth Planet. Sci. Lett.*, *265*(1–2), 246–255.
- Paden, J., T. Akins, D. Dunson, C. Allen, and P. Gogineni (2010), Ice-sheet bed 3-D tomography, *J. Glaciol.*, *56*(195), 3–11.
- Paterson, W. (1994), *The Physics of Glaciers*, 3rd ed., Pergamon, Oxford, U. K.
- Pattyn, F. (2003), A new three-dimensional higher-order thermomechanical ice sheet model: Basic sensitivity, ice stream development, and ice flow across subglacial lakes, *J. Geophys. Res.*, *108*(B8), 2382, doi:10.1029/2002JB002329.
- Reeh, N., C. Mayer, H. Miller, H. Thomsen, and A. Weidick (1999), Present and past climate control on fjord glaciations in Greenland: Implications for IRD-deposition in the sea, *Geophys. Res. Lett.*, *26*(8), 1039–1042.
- Reeh, N., H. Thomsen, A. Higgins, and A. Weidick (2001), Sea ice and the stability of north and northeast Greenland floating glaciers, in *Ann. Glaciol.*, *33*, 474–480.
- Rignot, E., and P. Kanagaratnam (2006), Changes in the velocity structure of the Greenland ice sheet, *Science*, *311*(5763), 986–990, doi:10.1126/science.1121381.
- Rignot, E., and K. Steffen (2008), Channelized bottom melting and stability of floating ice shelves, *Geophys. Res. Lett.*, *35*, L02503, doi:10.1029/2007GL031765.
- Rignot, E., S. Gogineni, W. Krabill, and S. Ekholm (1997), North and northeast Greenland ice discharge from satellite radar interferometry, *Science*, *276*(5314), 934–937.
- Rignot, E., S. Gogineni, I. Joughin, and W. Krabill (2001), Contribution to the glaciology of northern Greenland from satellite radar interferometry, *J. Geophys. Res.*, *106*(D24), 34,007–34,019.
- Thomas, R., E. Frederick, W. Krabill, S. Manizade, and C. Martin (2006), Progressive increase in ice loss from Greenland, *Geophys. Res. Lett.*, *33*, L10503, doi:10.1029/2006GL026075.
- Thomsen, H., N. Reeh, O. Olesen, C. Boggild, W. Starzer, A. Weidick, and A. Higgins (1997), The Nioghalvfjærdssjorden glacier project, north-east Greenland: A study of ice sheet response to climatic change, *Geol. Surv. Greenland Bull.*, *179*, 95–103.
- Vieli, A., and A. J. Payne (2005), Assessing the ability of numerical ice sheet models to simulate grounding line migration, *J. Geophys. Res.*, *110*, F01003, doi:10.1029/2004JF000202.
- Vogel, C. R. (2002), *Computational Methods for Inverse Problems*, Soc. for Ind. and Appl. Math., Philadelphia, Pa.
- D. Aubry and H. Ben Dhia, Laboratoire MSSMat, UMR 8579, CNRS, École Centrale Paris, F-92295 Châtenay-Malabry CEDEX, France.
- S. S. Kristensen, DTU-Space, Technical University of Denmark, Ørsted Plads, Bldg. 348, DK-2800 Kongens Lyngby, Denmark.
- E. Larour, Jet Propulsion Laboratory, California Institute of Technology, MS 157-316, 4800 Oak Grove Dr., Pasadena, CA 91109, USA.
- M. Morlighem and H. Seroussi, Jet Propulsion Laboratory, MS 300-331, 4800 Oak Grove Dr., Pasadena, CA 91109, USA. (helene.seroussi@jpl.nasa.gov)
- E. Rignot, Department of Earth System Science, University of California, Irvine, 3200 Croul Hall, Irvine, CA 92697-3100, USA.